Infrared Thermography for Monitoring of Freeze-Drying Processes: Instrumental Developments and Preliminary Results

HÅKAN EMTEBORG,[1] REINHARD ZELENY,[1] JEAN CHAROUD-GOT,[1] GUSTAVO MARTOS,[1] JÖRG LÜDDEKE,[2] HOLGER SCHELLIN,[3] KATHARINA TEIPEL[1]

[1]European Commission, Joint Research Centre, Institute for Reference Materials and Measurements, (IRMM) Retieseweg 111, B-2440 Geel, Belgium

[2]Martin Christ Gefriertrocknungsanlagen GmbH, An der Unteren Söse 50, D-37520 Osterode, Germany

[3]InfraTec GmbH Infrarotsensorik und Messtechnik, Gostritzer Str. 61-63, D-01217 Dresden, Germany

Received 13 February 2014; revised 3 April 2014; accepted 2 May 2014

Published online 5 June 2014 in Wiley Online Library (wileyonlinelibrary.com). DOI 10.1002/jps.24017

ABSTRACT: Coupling an infrared (IR) camera to a freeze dryer for on-line monitoring of freeze-drying cycles is described for the first time. Normally, product temperature is measured using a few invasive Pt-100 probes, resulting in poor spatial resolution. To overcome this, an IR camera was placed on a process-scale freeze dryer. Imaging took place every 120 s through a Germanium window comprising 30,000 measurement points obtained contact-free from −40°C to 25°C. Results are presented for an empty system, bulk drying of cheese slurry, and drying of 1 mL human serum in 150 vials. During freezing of the empty system, differences of more than 5°C were measured on the shelf. Adding a tray to the empty system, a difference of more than 8°C was observed. These temperature differences probably cause different ice structures affecting the drying speed during sublimation. A temperature difference of maximum 13°C was observed in bulk mode during sublimation. When drying in vials, differences of more than 10°C were observed. Gradually, the large temperature differences disappeared during secondary drying and products were transformed into uniformly dry cakes. The experimental data show that the IR camera is a highly versatile on-line monitoring tool for different kinds of freeze-drying processes. © 2014 European Union 103:2088–2097, 2014

Keywords: freeze-drying; lyophilization; infrared camera; thermography; infrared spetcroscopy; spatial resolution; water in solids; human serum; processing

INTRODUCTION

Freeze-drying is an excellent way of drying thermally sensitive materials and preserving thermally labile compounds. It is extensively used in the pharmaceutical and biotechnology industry to produce active pharmaceutical ingredients (e.g., small molecules and proteins), which then can be conveniently distributed and stored. Freeze-drying is also used in other sectors, for instance, in food industry (instant coffee), bacteriology (strain conservation), or chemical synthesis. Moreover, freeze-drying is a versatile means for processing of reference materials (RMs) for various application fields (e.g., clinical chemistry, food, and environment). Such RMs and especially certified RMs (CRMs) are important tools enabling laboratories all over the world to deliver accurate measurement results of demonstrated reliability.[1–3]

Considering the major efforts required for planning, processing, characterizing, and certifying a RM, the production of large and stable batches is preferred, so that the CRM is available for several years after production. To achieve the desired long-term stability of biological materials, removal of water is essential. Freeze-dried materials can be kept for many years for most matrix/analyte combinations, provided that they are stored at an appropriate storage temperature. Obviously, similar requirements apply for many pharmaceutical products with respect to stability and therefore freeze dryers are also widely used in pharmaceutical industry.

A freeze-drying cycle normally consists of the following three steps:

1. Freezing of the water present in the matrix at ambient pressure.
2. Sublimation or primary drying, whereby the water is evaporating from the solid ice in the material and captured on the condenser under vacuum.
3. Secondary drying where most of the remaining water is removed under hard vacuum and temperatures above 0°C.

During freezing, it is of interest to produce as large ice crystals as possible in the matrix.[4,5] Large crystals contribute to the formation of larger pores in the material to be dried, which results in a higher flux of water vapor from the material during primary drying. However, high freezing rates result in smaller ice crystals and smaller pores.[6] Hence, different ice crystal structures result in different flux of water vapor.

During sublimation, the chamber pressure is normally around 0.2 mbar (for the equipment used in this study) and the water vapor that leaves the ice is captured on the ice condenser placed under the freeze-drying chamber. When the sublimation step is approaching the end, the pressure is further reduced in the chamber to about 0.005 mbar, and the secondary drying is started. At the same time, the shelf temperature is further increased on the shelves so that most of the last free water can be removed from the matrix. Monitoring

Correspondence to: Håkan Emteborg (Telephone: +32-14-571-708; Fax: +32-14-571-548; E-mail: hakan.emteborg@ec.europa.eu)

Journal of Pharmaceutical Sciences, Vol. 103, 2088–2097 (2014)

of product temperature is achieved through point measurements using Pt-100 probes directly placed in the material. Some brands of freeze dryers also have so-called Lyo sensors that measure the resistivity in the material that is undergoing drying.

The spatial resolution is severely limited when using probes and moreover the probes are invasive, that is, in direct contact with the material. It is therefore difficult to judge how well the probes are characterizing the temperature of all the material that is loaded on a tray and if there are large differences between different areas on the tray. For applications involving drying in ampoules or vials, only a few units can be monitored when probes are used. In addition, when considering the limited sample amounts filled in vials (1 mL serum resulted in 80 mg dry mass in this study), the mass of the Pt100 probe itself of 160 mg adds additional mass to the monitored sample. This could potentially distort the measurement in comparison with vials that are not monitored with the probes. Measurements employing multiple probes systematically placed in the materials have been used to assess the spatial differences in temperature. Still, this approach is invasive, difficult, and unpractical and has inferior spatial resolution in comparison with a thermogram from an infrared (IR) camera.

A thorough literature search has not resulted in any findings of previous reports describing the combination of an IR camera with a freeze dryer. A US patent identifies IR imaging as a potential tool for monitoring of freeze-drying processes but it is suggested to place the IR camera inside the freeze-drying chamber.[7] Another report was found where a normal camera was suggested to be placed inside a freeze dryer.[8]

Other means of monitoring freeze-drying processes have been based on Raman spectroscopy and near-IR spectrometry.[9] There is also a commercially available system for monitoring of the water flux to the condenser using very small inductively coupled plasma atomic emission spectrometer. This so-called Lyo track system can effectively display the flux of water to the condenser during the primary and secondary drying as a function of time.[10] Finally, a thesis by Schneid contains a very comprehensive overview dealing with process analytical technologies for monitoring of freeze-drying processes.[11] However, none of these reported systems is actually monitoring the spatial temperature distribution on materials or between vials placed inside the freeze dryer.

In this paper, the technical details of the new coupling are presented alongside with results from a run of an empty system, one run of a system loaded with slurry made of cheese spiked with a bacterial protein toxin, and a run monitoring 136 vials of human serum during the whole freeze-drying cycle.

MATERIALS AND METHODS

An IR camera (VarioCAM; Jenoptik; InfraTec GmbH, Dresden, Germany) was mounted vertically on the chamber-roof of a freeze dryer (Epsilon 2-100D; Martin Christ, Osterode, Germany) where a hole of 70 mm diameter had been made in the roof of the freeze-drying chamber. Inside the chamber, a cut had been made in the radiation shield to allow a free view of the top shelf as can be seen in Figure 1. The IR camera recorded images of the material on the test tray with a high spatial and thermal resolution ($\sim 2 \times 2$ mm^2) and (50 mK). Obviously, only the top shelf was possible to monitor with the current system.

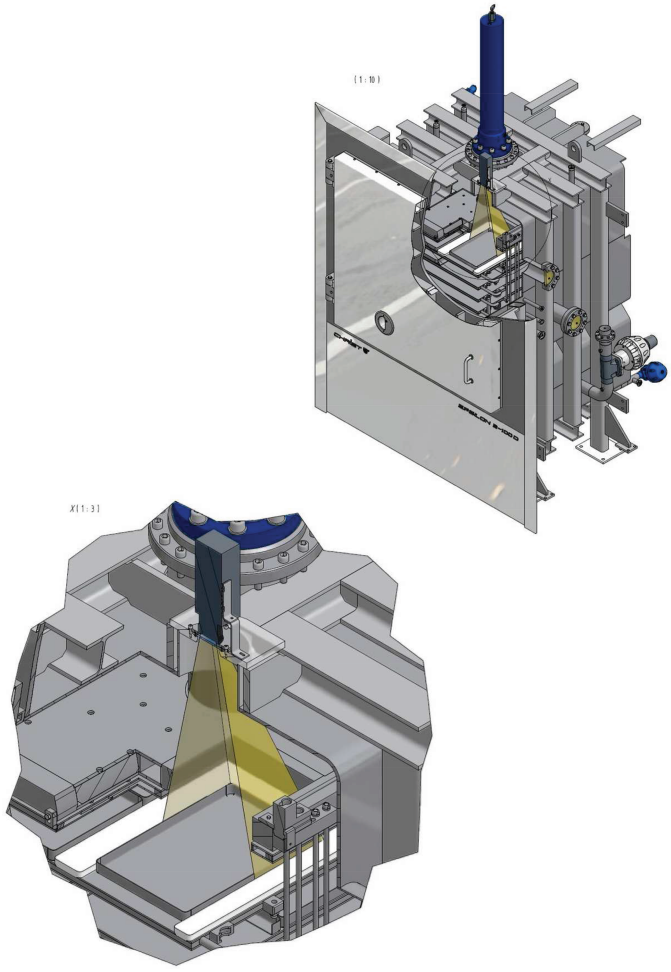

Figure 1. Integration of IR camera in freeze dryer. Top right shows the freeze-drying chamber in full and four shelves. Bottom left shows a magnification of area of interest with IR camera, viewing area, tray, and white holder for good alignment of the tray with the optics of the IR camera. During the operation of the freeze-drying programs, this holder had been removed.

Because the drying chamber is subjected to low pressures during operation, the opening was closed with a suitable window having sufficient IR transmission. Therefore, an 8-mm thick window made of Germanium of 10 cm diameter, which had been optically brightened and treated with a special coating, was placed over the opening. The Germanium window was resting on an O-ring and held in place by a steel ring that was fixed with eight screws. The Germanium window allows 80% transmission in the wavelength interval of interest (7.5–14 μm). The IR camera was equipped with a precision wide-angle lens with 64° flare angle. The lens was resting directly on the Germanium window and the camera itself was fixed to the freeze dryer with a z-shaped holder made from stainless steel. The resulting image was matching the size of a standard freeze-drying tray of 30 $\times$40 cm^2 placed on the top shelf. The stainless steel tray used for the cheese slurry had been coated with a black Teflon coating as to prevent excessive reflection in the IR part of the spectrum. The noncooled thermographic system VarioCAM achieves a geometric resolution of 640 $\times$ 480 IR pixels and delivers very reproducible results thanks to sophisticated calibration algorithms with a thermal resolution

of 50 mK. Because of the lens used and the distance to the observed tray, about 30,000 measurement points are displayed per tray. A time- or action-related recording is possible with the analysis and acquisition software IRBIS® 3. Data transfer from the camera to a laptop took place through an IEEE1394 fire wire interface that is able to handle the data flow possible in certain applications with speeds up to 50 Hz. For freeze-drying, a recording frequency of 50 Hz is exaggerated as the changes are relatively slow and gradual. The recording frequency was therefore set to one image per 120 s, which resulted in 2200 images during a full 73.3 h cycle except for the experiment of cooling down the empty tray that was based on one image every 30 s. The IRBIS® 3 software can reproduce these images at about 10 Hz in retrospect, which actually results in an IR film sequence of the entire freeze-drying cycle, cooling down, or another part of the freeze-drying program that is of interest. The software can plot the temperature as a function of time either in specific measurement points or as small areas in the form of circles or rectangles that can be freely selected in the IR image. For the vial experiment, 150 vials with 1 mL human serum were loaded in the freeze dryer. Out of these, 136 had no Lyo insert. Consequently, only these could be monitored with the IR camera with 136 such measurement points precisely placed in the image to display the temperature changes in each vial as a function of time.

Preparation of Cheese Slurry

Cubes of Tomme de Savoie cheese (Yenne, France) were finely milled using a kitchen model cutter (Moulinex, Moulinette-DP700, Ecully, France) only operated for few seconds per loading to avoid the creation of a thick paste. The finely cut cheese was then further dispersed in water (mixing ratio 1:1.5, m/m) using an Ultra Turrax DI25 basic (IKA Staufen, Staufen im Breisgau, Germany) operated at 8000 rpm to obtain a highly uniform, creamy homogeneous slurry. Finally, the slurry was spiked with *Staphylococcus aureus* enterotoxin A (Toxin Technology, Sarasota, Florida) at a concentration of 0.25 ng/g cheese. The tray that was used for this experiment was coated with a Teflon layer to avoid the very low emissivity of polished metal surfaces. The tray was loaded with 1 kg of cheese slurry (1 cm thick) and placed on the top shelf in the freeze dryer. This experiment can be considered typical for any bulk-mode operation. On the side of the tray, a strip of 130 × 50 mm^2 of masking tape had been placed whereby the shelf temperature could be readout using the IR camera as well. The masking tape was of 140 μm thickness consisting of a slightly creped paper and a rubber adhesive from Tesa Type 4316 (Brussels, Belgium). For the vial experiment, 150 vials were standing directly on the masking tape covering the shelf area monitored by IR camera. Further discussion concerning the masking tape can be found in the section describing emissivity.

The human serum originated from two patients diagnosed with the antiphospholipid syndrome (APS). The two patients underwent routine plasmaphoresis treatment. The plasma contains anti-β2 Glycoprotein I (anti-β2GPI) IgG autoantibodies, which are a relevant biomarker of the disease. After extraction, the plasma was clotted with a thrombin–$CaCl_2$ solution for 30 min at 37°C under agitation. After overnight incubation at 4°C, the material was filtered to eliminate fibrin. Sodium azide was added as conservation agent at a concentration of 0.2%. The resulting sera from both patients were blended and mixed with an equal volume of normal human serum. Then, it was stored at −70°C. The material was thawed at 4°C over the weekend before further processing. It was passed through a 0.22-μm filter and kept at 4°C before filling 1 mL into vials. The screw-cap vials were made of siliconized clear glass of 2.5 mL nominal volume supplied from ISO-GmbH (Bad Köningshofen, DE). The rack holding the vials was made of PVC that had been sprayed with black paint of high emissivity (Motip 04031; Motip Dupli, Wolwegen, NL).

Freeze-drying was accomplished by using a Martin Christ Freeze Epsilon 2-100D model. This equipment has five positions for normal Pt-100 probes and three positions for Lyo control probes to measure the temperature and resistivity directly in the material to be dried. One Pt-100 probe and one Lyo control probe were placed in the cheese slurry that was monitored by IR camera. A second Pt-100 probe was placed in another tray filled with cheese slurry that was placed on another shelf just below. In total, 48 trays of 30 × 40 cm^2 were loaded in this system for the bulk experiment. In the vial experiment, the probes were placed in vials standing on shelves below the one monitored by the IR camera.

Process monitoring data from the freeze dryer is given in Table 1 for cross-matching with temperatures measured with the IR camera. Water content was measured using a Sartorius MA150 oven balance (Göttingen, Germany) on approximately 6 g of the dried cheese material taken from different locations on the trays. For water content in the serum, vaporization coulometric Karl Fischer titration was employed (Metrohm, Herisau, Switzerland).

RESULTS AND DISCUSSION

Three types of observations will be described here that have been obtained with this new instrumental combination. In the first instance, the temperature distribution on the shelf and on an empty tray had to be checked. Second, the whole freeze-drying process of bulk-mode operation on cheese slurry was monitored using IR thermography. Finally, monitoring of 136 vials of human serum was also performed to highlight the relevance of this coupling for the pharmaceutical field. Each part of the cycle during empty and charged runs is discussed more in detail below. To understand the implications, some general remarks about freeze-dryer designs and a discussion about emissivity are necessary before presenting the detailed results.

Freeze-Dryer Designs

Normally, inhomogeneous temperature distribution on the shelves as such does not exist during static steps in the freeze-drying program when the temperature is kept constant. The manufacturer is checking this at the time of manufacturing and site acceptance tests by placing probes at different positions on the shelves with an accepted difference of ±1°C. Moreover, the cooling/heating liquid (Syltherm, silicone fluid; DOW, Midland, Michigan) flowing through the shelves and radiation shield is pumped in parallel through the shelves and not in series. (The freeze dryer used in this experiment has six shelves and one radiation shield in the chamber, 6 + 1). Serial connection of the shelves means that the cooling liquid flows through the shelves one after the other. In a parallel arrangement, each shelf is fed separately from the cooling liquid supply with the same flow rate. This arrangement together, with the specially designed

Table 1. Different Temperature Readouts at Different Time Intervals in the Freeze-Drying Program Using Probes, IR Camera, or Freeze-Dryer Control System

Product and Figure Reference	Time (h) and Pressure[a] (mbar)	Product Temperature[b] Pt-100 (°C)	Resistivity, Lyo RX (%)	IR Camera, Shelf/Tray/Product (°C), Average (Minimum/ Maximum)[c]	Temperature Difference (°C)[d]	IR Camera Shelf[e] (°C), Average Minimum/ Maximum)	Freeze Dryer, Actual Shelf Temperature (°C)
Shelf (Fig. 2b)	0.25 (amb.), D	–	–	−1.8 −4.9/0.2	5.1	−1.4 −1.7/−1.0	−2
Shelf (Fig. 2c)	0.75 (amb.), D	–	–	−38.5 −41.8/−36.1	5.7	−39.8 −40.5/−39.0	−37
Shelf (Fig. 2a)	30 (0.2), S	–	–	−11.0 −11.7/−10.1	1.8	−11.2 −11.6/−10.7	−10
Shelf	68 (0.003), S	–	–	19.5 19.0 / 19.9	0.9	19.6 19.3 / 20.0	20
Tray (Fig. 2d)	0.25 (amb.), D	–	–	2.6 −2.6/5.6	8.2	−0.8 −1.2/−0.4	−3
Cheese (Fig. 2e)	1.4 (amb.), S	−34; −34; −30	74	−10.3 −29.5/0.3	29.8	−36.2 −36.8/−35.4	−40
Cheese (Fig. 2f)	30 (0.2), S	−13; −11; −10	98	−9.8 −18.7/−5.7	13.0	−11.6 −12.3/−11.2	−11
Cheese (Fig. 2g)	68 (0.006), S	17; 15; 16	98	16.2 15.4/18.1	2.7	19.2 18.8/19.7	20

[a] amb., ambient presssure; D, dynamic part of program; S, Static part of program.
[b] Temperatures obtained from the probes as given in legend in Figure 3a.
[c] Readout of average, maximum, and minimum in selected rectangles on masking tape placed on shelf in empty run using IRBIS® 3, $\varepsilon = 0.9$. Average maximum and minimum was measured on the whole tray when loaded with cheese slurry, with $\varepsilon = 0.95$.
[d] Temperature difference is referring to the difference of maximum and minimum values for the data column "shelf/tray/product."
[e] Readout of average, maximum, and minimum using IRBIS® 3 on masking tape denoted R1 (in Fig. 2a) placed next to freeze-drying tray, $\varepsilon = 0.9$.

interior pathway for the cooling liquid, leads to a more uniform temperature distribution on and between the shelves. The Martin Christ freeze dryer has consequently seven separate supplies from the same cooling liquid reservoir. Consequently, with the excellent spatial and thermal resolution obtained by recording IR images of the shelf during an empty run, the absence of large temperature deviations on the shelves could be confirmed for static steps of the program as shown in Figure 2a. Nevertheless, during dynamic steps such as rapid cooling down, temperature differences of approximately 5°C could be observed as shown in Figures 2b and 2c. When adding an empty tray to the empty system, differences of more than 8°C could be observed on this tray during cooling down (freezing step), which was also partially depending on the actual physical contact between tray and shelf. The relative temperature differences on the shelf were basically transferred to the tray (Fig. 2d).

Emissivity

Emissivity (ε) of a material is the relative ability of its surface to emit energy by radiation. It is the ratio of energy radiated by a particular material to the energy radiated by a perfect black body emitter at the same temperature.[12] In general, the blacker and duller a material is, the closer its emissivity is to 1.0. Because of the fact that the shelf is made of highly polished steel (Material code 1.4404, similar to ANSI 316 steel Ra value <0.4 μm), several implications occur when trying to monitor the shelf temperature directly with an IR camera. First, the emissivity of metals is very low, which gives erroneous temperature readouts. Second, the low emissivity makes the steel plate act as an IR mirror. If no action would be taken to increase the emissivity, one would effectively only be able to see the reflection of the lens of the IR camera and not be able to monitor the shelf temperature correctly. Emissivity tables are published for many materials but it should be noted that emissivity can change slightly with texture, viewing angle, color, and actual temperature. For the purpose of this study, to be able to measure the shelf temperature over a large area, the shelf was covered with seven parallel stripes of masking tape of 140 μm thickness. The masking tape was made of a slightly creped paper and a rubber adhesive Tesa type 4316 (Brussels, Belgium). The bands were placed very close to each other to provide an even surface as possible with uniform emissivity. Still, it can be seen in Figures 2b and 2c that the stripes were not perfectly aligned, as some very narrow horizontal lines can be seen in the IR images. An ε value of 0.90 was found for masking tape that has consequently been applied for all measurements of the tape with the IR camera.[13] By placing the tape, much higher emissivity of the shelf surface was obtained and it completely eliminated the problem of IR reflection. Fortunately, most biological materials have high emissivity.[14] Hence, biological materials that are viewed using the IR camera in this coupling will have reliable temperature readouts even without any correction for the emissivity. In this study, a value of $\varepsilon = 0.95$ has been applied to all measurements of the cheese slurry and human serum. The IRBIS® 3 software has a built-in module for emissivity corrections.

Concerning the interpretation of thermograms, Figures 2a–2g and later in the text, it should be noted that the color coding for a certain temperature is only valid per figure as given on the color-coded temperature scale to the right in each thermogram. Moreover, the wider the temperature range is, the smoother the temperature differences appear to be. The opposite is true for images where a narrow temperature range is shown as individual pixels become visible. All thermograms for the cheese bulk experiment have the same physical size to simplify

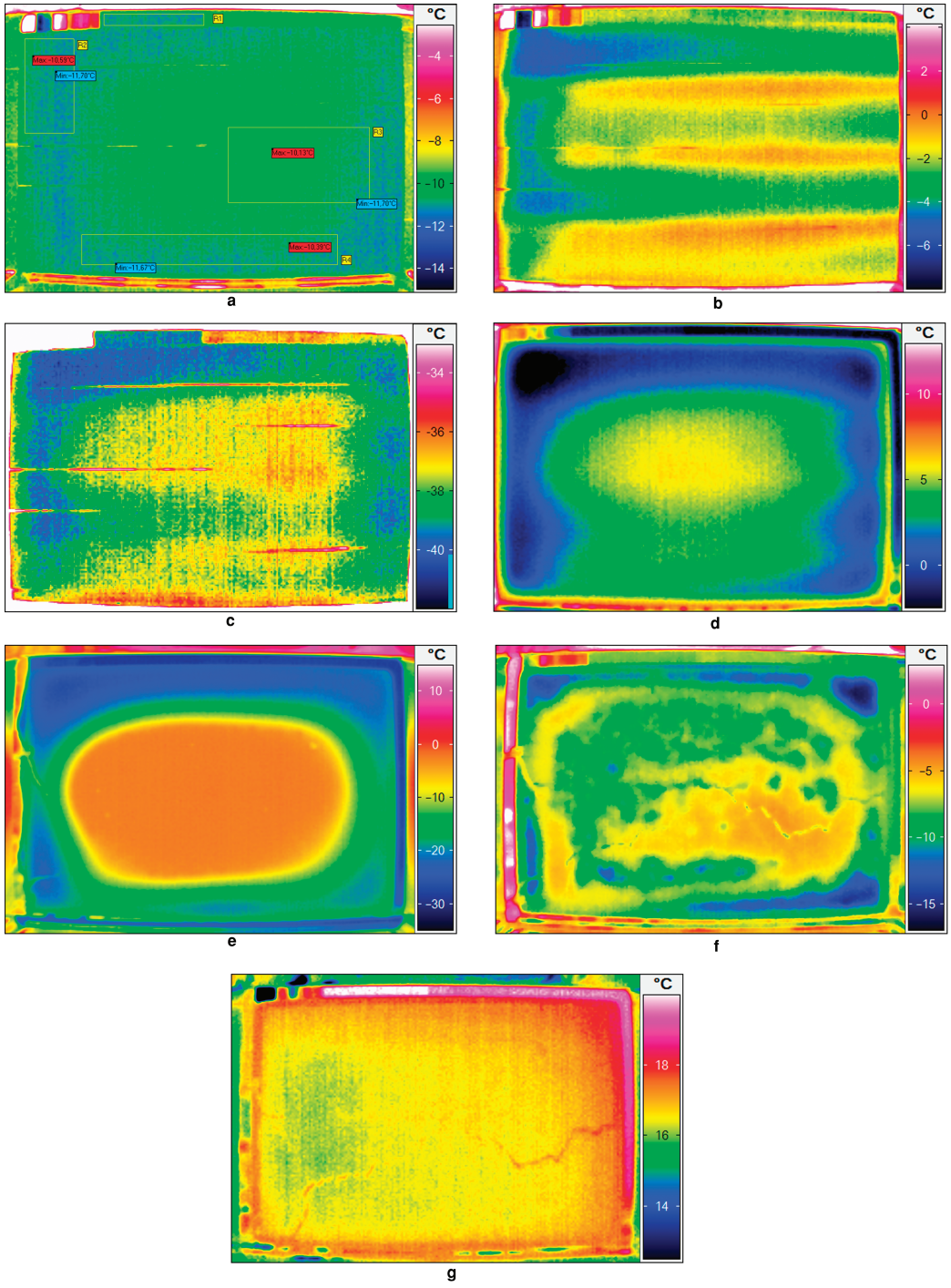

Figure 2. (a) Thermogram of empty run of shelf after 30 h of operation. Rectangle R1 shows the area of masking tape used to measure the shelf temperature using the IR camera in the presence of a tray. R2, R3, and R4 display maximum and minimum temperatures of each area, respectively, confirming an even temperature distribution on the shelf. For more information, cross-correlation with Table 1 is necessary, $\varepsilon = 0.90$. (b) Thermogram of empty run of shelf after 15 min where temperature differences can be observed between inside walls and central parts of the channels where the silicon oil is flowing. Thin horizontal lines are narrow gaps between the stripes of masking tape. For more information, cross-correlation with Table 1 is necessary, $\varepsilon = 0.90$. (c) Thermogram of empty run of shelf after 0.75 h operation at the end of cooling down where temperature differences can still be observed between inside walls and central parts of the channels. Thin horizontal lines are narrow gaps between the stripes of masking tape, $\varepsilon = 0.90$. (d) Thermogram of empty run with tray after 15 min. Top left corner is coldest, which suggests the best contact with the shelf, $\varepsilon = 0.90$. (e) Thermogram of run with cheese slurry after 1.4 h of operation in the freezing step. Central part is still not frozen and Pt-100 probe and Lyo control are visible to the left as light-green threads in the blue background, $\varepsilon = 0.95$. (f) Thermogram of run with cheese slurry after 30 h of operation in the sublimation step. Large temperature differences are apparent in different parts of the tray. Cracks in the slurry are also visible suggesting that certain areas are approaching dryness, $\varepsilon = 0.95$. (g) Thermogram of run with cheese slurry 68 h into the program in the secondary drying step; some water is still leaving the material because the temperature on the material is lower than the shelf. Pink/white horizontal bar on top left is rectangle of masking tape; R1 in Figure 2a used to monitor the shelf temperature, $\varepsilon = 0.95$.

comparisons. For the vial experiments, different magnifications have been used. The camera can only measure down to −40°C. Some data in Table 1 and Figure 2c are reported to be below −40°C. This is possible because the temperature has been recalculated using an emissivity of 0.9. For all thermograms displayed, the door of the freeze dryer is located to the left in each thermogram. The cooling liquid inlet to the shelf is located to the bottom left in each thermogram.

In case of the cheese slurry, no masking tape remained on the shelf as soon as a tray was placed on the shelf to maximize energy transfer from the shelf to the tray. For the vial experiment, the masking tape remained on the shelf to be able to monitor the shelf temperature around each vial.

Individual Empty Runs of Shelf and Tray

Temperature differences could indeed be observed on the shelf during the cooling down or freezing step as the cooled silicon oil starts to flow through the shelves. In Figure 2b, the internal walls in the shelf can be observed as warmer areas separating the channels inside the shelves whereby the silicon oil is forced to flow in a zigzag pattern. For this experiment, a maximum temperature difference of 5.1°C was found for the shelf during rapid cooling down (freezing step). This temperature difference is occurring for a period of approximately 1 h during cooling down, which at least partially affects the freezing process (Fig. 2e; Table 1). Later in static parts of the freeze-drying program, the differences are only around 1.5°C as shown in Figure 2a. To check the temperature distribution on an empty tray, the same tray used for the cheese slurry was subjected to the cooling step in the freeze dryer. It could be observed that the temperature differences present on the shelf were partially translated to the tray placed on the shelf as depicted in Figure 2d, especially with respect to the coldest top left corner. The largest temperature differences observed on the tray were 8.2°C that could be directly attributed to the good (or bad) contact with the shelf as discussed further below and the temperature differences on the shelf itself during the dynamic cooling down process (see Table 1 after 0.25 and 0.75 h, respectively). In addition, the tray may flex and bend slightly when large temperature differences exist locally because of the thermal expansion/contraction of the metal as a function of temperature. In the static situations in all parts of the freeze-drying program, the differences on the shelf were much smaller as already mentioned.

Monitoring of a Run with Cheese Slurry (Bulk Mode)

Results for experiments of lyophilizing cheese are reported here, as part of a feasibility study for producing a candidate CRM for *Staphylococcus aureus* enterotoxin A, which is a protein toxin associated with food poisoning outbreaks. The Lyo control probe RX sensor was employed to measure the resistivity in the material, but it was also providing additional temperature data as given in Table 1 (obtained from Figure 3a). During the cycle, the observed temperature on the masking tape adjacent to the tray was in very close agreement with the shelf temperature monitored by the freeze dryer. All the graphical traces of shelf temperature, probe temperatures, resistivity, vacuum, and so on are displayed in Figures 3a (cheese) and 3b (serum), respectively, whereas numerical data can be found in Table 1 for the bulk experiment.

Freezing Step

Figure 2e (image 41; 1.4 h into the program) is showing freezing of the cheese slurry, where the top left was frozen first and much colder (−29.5°C) than the rest of the slurry and it is clear that the colder areas on the tray have a better contact with the shelf but also because the shelf is actually colder in this area during the dynamic cooling-down process (Figs. 2b to 2d). The difference was 29.8° from −29.5°C to 0.3°C. The probes are also visible to the left in this IR image. The Lyo control can be seen to the left in the middle of the tray and the Pt-100 probe to the bottom left. Table 1 lists the average, maximum, and minimum values recorded for this stage with the camera, probes, and freeze dryer internal readouts.

Sublimation Step, Primary Drying

Relatively soon after the sublimation step had started, it could be observed that large islands of relatively colder areas were present in the cheese slurry on the tray (Fig. 2f). Local differences of 13°C (between −19°C and −6°C) could be observed on the surface of the cheese slurry. Figure 2f is taken 30 h into the program and it reveals that some areas are warmer than the shelf temperature and that others are much colder, and finally some parts approach dryness because the material starts cracking. This is not caused by an inhomogeneous temperature distribution on the shelf during sublimation. Table 1 and Figure 2a show a maximum difference of 1.8°C in the sublimation step for the empty run (shelf only). The tray also exhibits a relatively even temperature distribution in static parts of the program as checked at the end of the freezing step. In Table 1, one can also see that the Lyo control sensor reads 98% resistivity that indicates dryness in this point. As mentioned above, it must be noted that the Lyo control sensors and Pt-100 probes have very limited spatial resolution. Although the IR camera is recording an image of the surface with a spatial resolution of about 2×2 mm^2, it is also possible to discern that the inside of the cake is not much colder than the surface as the temperature difference should otherwise be much visible inside the cracks. In fact, it is even possible to see the bottom of the Teflon-coated tray as the cracks widen up during the drying cycle. Temperature differences of more than 6°C persist for 11 h during the freeze-drying cycle (from 24–35 h into the program). This information is also confirmed when inspecting product temperature traces in Figure 3a and Table 1 for this time interval.

The explanation for these temperature differences is probably because of different ice crystal sizes caused by nonuniform freezing conditions in different parts of the tray (Fig. 2e). Possibly ice crystals are different in the areas that froze first, making it more difficult for these parts of the material to dry as easily as in the central parts of the tray that had slower freezing (with possibly larger crystals). The manufacturer is making every effort to produce trays and shelves that are as flat as possible, but still this non-uniform drying probably takes place because of temperature differences during the dynamic cooling-down process. The slurry was very homogeneous and equally thick all over the tray. Consequently, it cannot be inferred that it was denser or more compact in the colder areas on the tray. What is also important to note is that the final result was evenly thick, evenly dry, and brittle cake, because at the final stage of sublimation, no major temperature differences exist any longer. At the end of the sublimation phase, it seems that the colder areas are more concentrated toward the inside of the freeze dryer

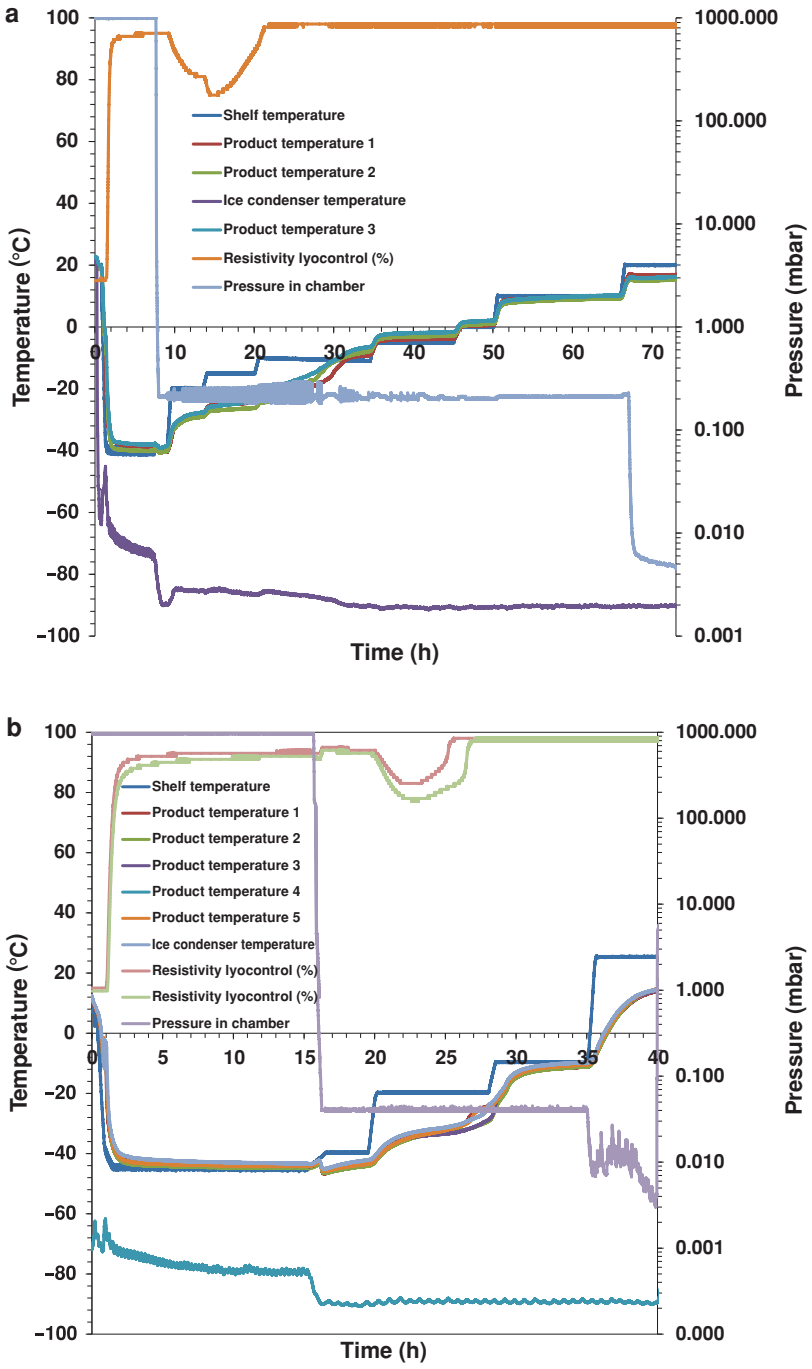

Figure 3. (a) Graphical output of the freeze-drying program for the cheese slurry as monitored by the freeze dryer. (b) Freeze drying program of human serum in vials as monitored by the freeze dryer. For both materials the traces for shelf temperature, product temperature and vacuum are most important.

possibly inferring a wall–door effect because areas closer to the wall and door are exposed to more thermal radiation energy from the outside.

Secondary Drying

Finally, when the system switches from sublimation to secondary drying, the large temperature differences no longer present as depicted in Figure 2g (68 h into the program). It is interesting to note that as the pressure drops and more energy is injected into the shelf, the material becomes colder than the shelf, probably because of evaporation of the last free water. The difference at this stage is approximately 2.7°C (from 15.4°C to 18.1°C), whereas the shelf has a temperature of about 19.2°C. The moisture content after a completed cycle was 2.4% (m/m) for cheese from the center of the thermographed tray and 2.1% and 2.5% closer to the edges. The second tray placed in the freeze dryer filled with cheese slurry had 2.3% (center) and 2.0% (edge) (second tray not monitored with the IR camera just placed on a shelf below). The overall mass loss from the cheese was about 43% (m/m).

 DOI 10.1002/jps.24017

Monitoring of a Run Human Serum in Vials

Freezing Step

During loading of the vials, the shelves were kept at +8°C. After all the 2860 vials had been filled and the freeze dryer was fully loaded, the drying program was started. The initial freezing process from 0°C to −10°C was rather uniform with a maximum temperature difference of about 4°C between the vials as shown in Figure 4a. As the freezing step proceeded, the temperature suddenly increased again to just below 0°C. After less than 10 min at 0°, the serum froze permanently with a rapid temperature drop to below −30°C. After this, the serum slowly reached −40°C with a temperature difference between vials of about 8°C in this segment. The pressure was thereafter reduced in the chamber that resulted in a dip in the temperature as can be seen at 16 h in Figures 3b and 4b. Note that temperatures below −40°C are calculated by the software of the IR camera because of the correction for emissivity of the serum, ε = of 0.95 or the masking tape, ε = 0.90. The very large differences in temperature observed for the freezing step occurring in the bulk-mode operation were not observed for the vials, although an effect of microthawing was observed. As serum contains proteins and salts, the freezing point will be below 0°C. At a certain point, there is crystallization (freezing) of water. At that time, the water freezes out, and the temperature goes up to the freezing point of water. It is possible to prevent this freezing behavior by shock freezing of the vials or loading on shelves that are at −20°C or below. However, these options were not possible at the time of processing.

Sublimation Step, Primary Drying

Figure 5a is showing all 150 vials in the sublimation step after 20.9 h of drying (for cross-reference to Figs. 3b and 4b). The serum is visible as dark-blue spots in all vials that do not have a Lyo insert. Considering that the opening of the vial has a diameter of 7 mm, about 6–9 pixels properly account for the central part of the vial and serum visible to the IR camera. In Figure 5b, a magnified area of the vials is shown with the points of measurement shown per vial (also at 20.9 h). In total, 136 such data points form the basis for the temperature readouts as a function of time as shown in Figures 4a–4c. A small circle integrating 4–6 pixels was also tested. It turned out that there was no difference in the overall temperature differences between the vials as displayed in Figures 4a–4c using a spot measurement or averaging a small circle. The primary drying proceeded slowly during 20 h from −45°C to −5°C as shown in Figure 4b. A detail of the temperature readout from the 136 vials is shown between 24 and 30 h in Figure 4c. It is interesting to note that at 27.7 h, the temperature of the shelf is shifted from −20°C to −10°C as given in Figure 4b. Just before that, the surface of the serum in the vials had reached temperatures between −21°C to −15°C. This observation is analogous to what was seen for the bulk application of cheese in Figure 2f where certain areas had indeed a temperature above the shelf temperature as confirmed both with the IR camera and the probes. Very shortly after the temperature of the shelf was shifted, the temperature difference in the vials diminished as the subsequent phase at −10°C commenced. It is also

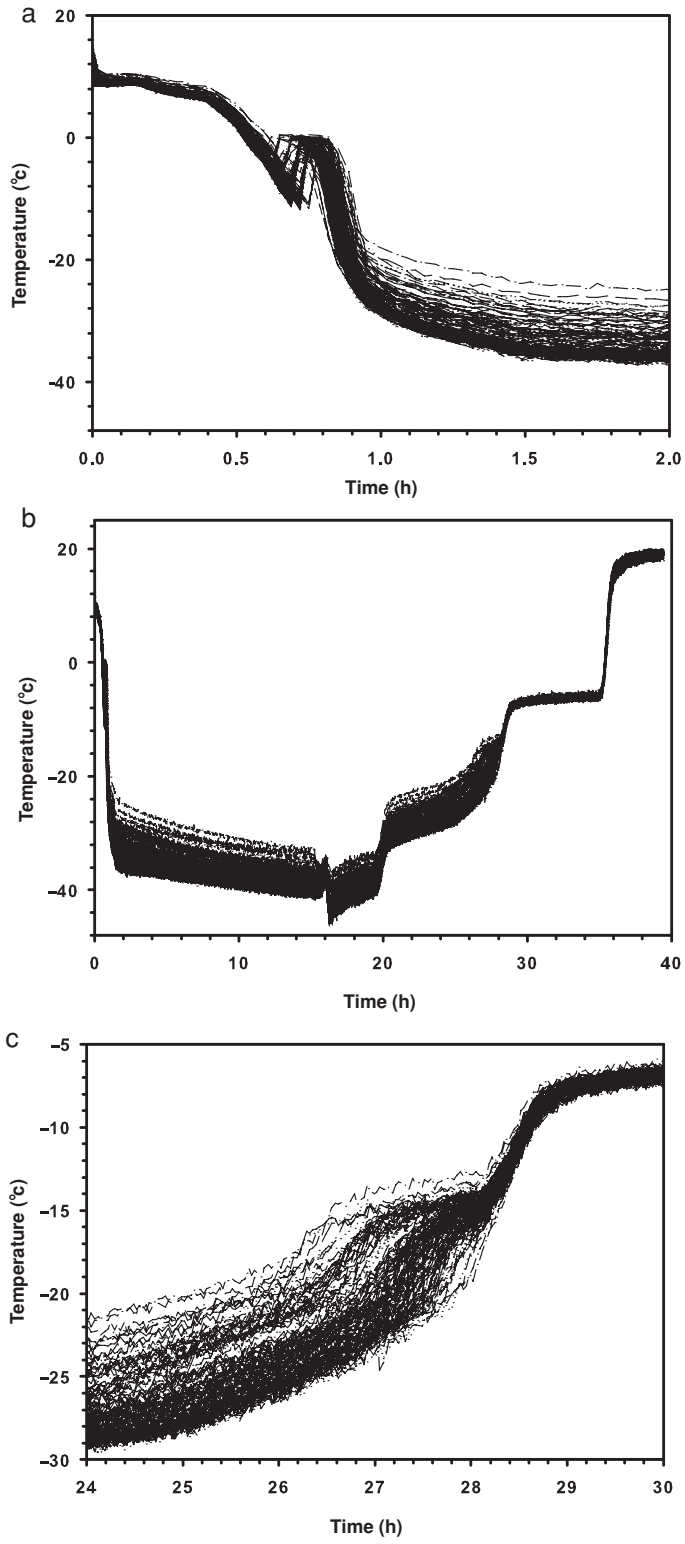

Figure 4. All the traces depicted in this figure represent temperature as a function of time with readings from 136 vials using the IR-camera every 2 min. Cross-correlation of product temperatures with Figure 3b is possible. (a) Freezing step of human serum. (b) Whole freeze-drying cycle of human serum. (c) Selected segment of the sublimation step of human serum.

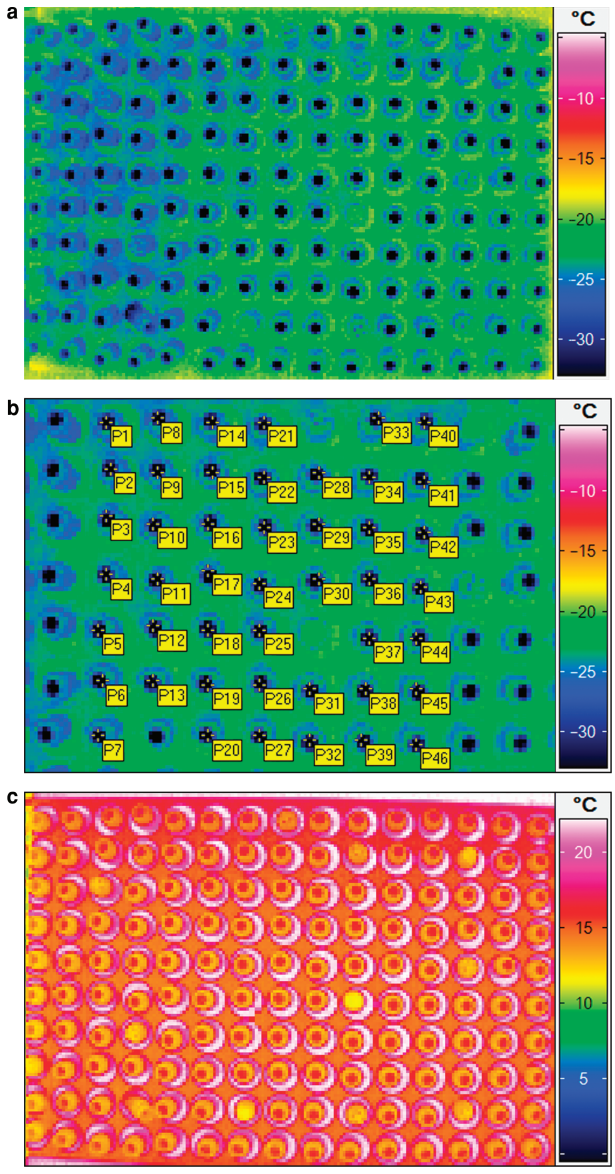

Figure 5. (a) Thermogram of 150 vials filled with human serum in the sublimation step after 20.9 h. The serum is visible as dark-blue spots. Occasionally, the vial is fitted with a Lyo-insert; in such cases, the vial is green and the temperature of the serum cannot be measured. The shelf temperature can easily be measured around each vial. (b) Thermogram of 70 vials filled with human serum in the sublimation step after 20.9 h with assigned measurement points. The serum is visible as dark-blue spots. (c) Thermogram of 150 vials filled with human serum in the secondary drying step after 36.6 h. The serum is visible as red spots. Occasionally, the vial is fitted with a Lyo-insert; in such cases, the vial is yellow and the the temperature of the serum cannot be measured.

interesting to observe the changing slope of the individual temperature readings. More work is needed to understand these processes that are outside the scope of the current paper.

Secondary Drying

In Figure 5c, the vials are shown in secondary drying after 36.6 h of drying as a cross-reference to Figures 3b and 4b. The shelf temperature can be read around every vial and is seen as white half-circles. The serum itself is visible as red spots of a lower temperature. An interesting observation can be made for the secondary drying step because the difference between the temperature readout for the probes as given in Figure 3b is rather different from the data shown in Figure 4b. The probes tend to lag substantially in the temperature readout in contrast to the results from the IR image. It may be a result of very poor thermal conductivity because the probes (having a mass of 160 mg) are fixed in a porous structure of 80 mg of dry serum with hollow spaces in hard vacuum. Because of this, it is doubtful whether the probe readout is really correctly reflecting the temperature of the dried serum. The IR camera is measuring the surface temperature. On the contrary, the probe is not measuring the temperature at the sublimation interface either, because it is completely immersed in the almost dry product and has dimensions that are much thicker than the sublimation front. Again, more work is needed to understand what is causing this difference. Finally, it is also important to verify that the emissivity corrections are correct to possibly correlate better with the readout from the probes. The water content in the serum was 1.1% (m/m) as determined by Coulometric Karl Fischer titration after vaporization at 110°C. The mass loss from the serum was 92.4% (m/m).

CONCLUSIONS

Infrared thermography offers exciting new possibilities for monitoring of freeze-drying processes. It could be shown that IR thermography provides superior spatial and thermal resolution concerning the measurement of a freeze-drying cycle in contrast to traditional means such as Pt-100 probes. On the basis of the data from these first experiments (empty system; vials containing human serum and cheese slurry containing a bacterial protein toxin), it has to be concluded that at certain time points in the process, the drying behavior is much less uniform than previously known only using Pt-100 probes for monitoring. This new application should also allow an even better design of shelves and trays in freeze dryers in the future and it could perhaps provide a better understanding of how different materials are drying during the different freeze-drying steps.

Prices of IR cameras have dropped substantially in the last years and this coupling is not out of reach for operators of freeze dryers of existing systems as retrofitting should be technically feasible. There is a distinct advantage to keep the IR camera outside the chamber because it makes it possible to use this technology for freeze dryers that have SIP/CIP options, that is, thermal sterilization and cleaning in place with steam (125°C and 2.1 bar). Manufacturing, data transfer, and control of the internal temperature of the camera and its microbolometer are also easier if the IR camera is kept outside the chamber.

ACKNOWLEDGMENTS

Hendrik Emons (IRMM) is acknowledged for supporting this idea already at the time of designing the freeze dryer. John Seghers (IRMM) is acknowledged for helping in preparing cheese slurries. Rohan Willis from the University of Texas Medical Branch (UTMB, Texas) is acknowledged for providing the serum material derived from APS patients.

The European Commission does not endorse any special brand or make of equipment.

REFERENCES

1. Certification report. 2009. Certification of mass fractions of aflatoxin B_1, B_2 and G_1 in compound feeding stuff. Certified reference material ERM®—BE376, EUR 23817 EN. ISBN 978-92-79-12354-2.
2. Certification report. 2008. Certification of proteins in the human serum Certified Reference Material ERM®—DA470k/IFCC, EUR 23431 EN. ISBN 978-92-79-09490-3.
3. Certification report. 2010. Certification of cystatin C in the human serum reference material ERM®—DA471/IFCC, EUR 24408 EN. ISBN 978-92-79-07562-9.
4. Konstantinidis AK, Kuu W, Otten L, Nail SL, Sever RR. 2011. Controlled nucleation in freeze-drying: Effects on pore size in the dried product layer mass transfer resistance and primary drying rate. J Pharm Sci 100:3453–3470.
5. Patapoff TW, Overcashier DE. 2002. The importance of freezing on lyophilization cycle development. BioPharm Int 15:16–21.
6. Petzold G, Aguilera JM. 2009. Ice morphology: Fundamental and technological applications in foods. Food Biophys 4:378–396.
7. Zane AA. 2012. Patent US 2012/0057018A1.
8. Böttger F, Häuptle M. 2011. Patent US 2011/0099836A1.
9. De Beer TRM, Vercuysse P, Burggraeve A, Quinten T, Ouyang J, Zhang X, Vervaet C, Remon JP, Bayens WRG. 2009. In-line and real-time process monitoring of a freeze dying process using Raman and NIR spectroscopy as complementary process analytical technology (PAT) tools. J Pharm Sci 98:3430–3446.
10. Mayeresse Y, Veillon R, Sibille PH, Nomine C. 2007. Freeze-drying process monitoring using a cold plasma ionization device. PDA J Pharm Sci Technol 61:160–174.
11. Schneid SC. 2009. Investigation of novel processing analytical technology (PAT) tools for use in freeze drying processes. Ph.D. Thesis. Erlangen, Germany: Friedrich-Alexander Universität Erlangen-Nürnberg.
12. Ingle JD, Crouch SR. 1988. Spectrochemical analysis. Prentice-Hall, Englewood Cliffs, NJ, 90–91.
13. Gustavsen A, Berndahl P. 2003. Spectral emissivity of anodized aluminium and the thermal transmittance of aluminium window frames. Nordic J Building Phys 3:1–12.
14. Porter W, Gates DG. 1969. Thermodynamic equilibria of animals with environment. Ecol Monog 39:227–244.